https://ntrs.nasa.gov/search.jsp?R=19910021323 2020-03-19T16:57:27+00:00Z

IN-46-CR
39567
p 21

PROGRESS REPORT ON

THE EFFECT OF CLOUDS ON THE EARTH'S RADIATION BUDGET

by

DANIEL ZISKIN

and

DARRELL F. STROBEL

Principal Investigator

Department of Earth and Planetary Sciences
Department of Physics and Astronomy

The Johns Hopkins University

Baltimore, MD 21218

NASA Grant: NAG 5 1476

September 24, 1991

(NASA-CR-188804) THE EFFECT OF CLOUDS ON THE EARTH'S RADIATION BUDGET Progress Report (JHU) 21 p
CSCL 04A

N91-30637

Unclas
G3/46 0039567

The Effect of Clouds on the Earth's Radiation Budget

ABSTRACT

The radiative fluxes from ERBE and the cloud properties from ISCCP over Indonesia for the months of June and July of 1985 and 1986 were analyzed to determine the cloud sensitivity coefficients. The method involved a linear least-squares regression between co-incident flux and cloud coverage measurements. The calculated slope is identified as the cloud sensitivity. It was found that correlations between the total cloud fraction and radiation parameters were modest. However, correlations between cloud fraction and IR flux were improved by separating clouds by height. Likewise, correlations between the visible flux and cloud fractions were improved by distinguishing clouds based on optical depth. Calculating correlations between the net fluxes and either height or optical depth segregated cloud fractions were somewhat improved. When clouds were classified in terms of their height and optical depth, correlations between all the radiation components were improved. Mean cloud sensitivities based on the regression of radiative fluxes against height and optical depth separated cloud types are presented. Results were compared to a one-dimensional radiation model with a simple cloud parameterization scheme.

I. INTRODUCTION

The Earth's Radiation Budget (ERB) is the exchange of radiant energy between the earth and space. The components of the ERB are the solar heating and the radiative cooling of the earth. Sustained changes in these components brought on by external forcing, such as increasing concentrations of 'greenhouse gases', could affect the climate. Furthermore, changes in one aspect of the climatic system will also force other components to change. Thus there is a feedback loop between the external force and the climate system. For example, the external forcing could cause a change in cloudiness. The change in cloudiness would affect the net radiation at the Top-of-the-Atmosphere (TOA), which in turn affects climate. The clouds would serve as a feedback mechanism. At present, clouds represent the largest source of uncertainty regarding how the climate will respond to external forcing [*Arking*, 1991]. Clouds potentially could act as a positive or negative feedback to the global climate, or their overall effect could be negligible. Although their effect on climate remains undetermined, we attempted to measure the effect clouds have on the components of the Earth's Radiation Budget (ERB).

In general, three measurements must be made in order to determine the ERB at any location: the solar input ($S_\odot$), the reflected sunlight (SW), and the Out-going Long-wavelength Radiation (OLR). The ERB at any time and place can then be defined to be:

$$N = S_\odot \mu - SW - OLR, \tag{1}$$

where N is the NET radiative flux and μ is the cosine of the solar zenith angle. By measuring both SW and $S_\odot$ and calculating μ, the total albedo can be defined:

$$\alpha_T \equiv \frac{SW}{S_\odot \mu}. \tag{2}$$

The heating term, Q, is expressed as:

$$Q = S_{\odot}\mu \times (1 - \alpha_T). \tag{3}$$

Both α_T and OLR are strong functions of fractional cloud coverage. Typically OLR also depends on cloud height, and the albedo depends on the optical depth (OD) of the cloud. In this paper we present how changes in fractional cloud coverage are related to changes in the components of the ERB. In particular, how does the height and OD of clouds affect their interactions with the radiation flux at the TOA.

The net cloud sensitivity (δ), which is a measure of how sensitive the components of the ERB are to changes in cloud coverage, can be expressed as:

$$\delta \equiv \frac{\partial N}{\partial f} = -S_{\odot}\mu \frac{\partial \alpha_T}{\partial f} - \frac{\partial OLR}{\partial f}, \tag{4}$$

where the first term on the right-hand side is referred to as the short-wavelength sensitivity coefficient ($G_S \equiv -S_{\odot}\mu \frac{\partial \alpha_T}{\partial f}$). The second term is known as the long-wavelength sensitivity coefficient ($G_L \equiv \frac{\partial OLR}{\partial f}$) [*Schneider*, 1972]. G_S and G_L describe the effect a change in cloudiness has on the earth's radiation field at the TOA. G_S is responsible for the 'albedo effect'. Since clouds generally reflect more light than the surface, increasing cloudiness reduces Q (the heating). G_L contributes to the 'greenhouse effect'. This is the tendency for clouds to reduce the radiative cooling of the Earth's surface. Thus clouds tend to cool the earth by the albedo effect, while also warming the earth by the greenhouse effect. The overall effect of these conflicting influences is uncertain.

We used satellite data to calculate G_L, G_S and δ. Variations between different cloud types has a large effect on the cloud sensitivity. When all clouds are treated equivalently, it is difficult to draw any conclusions since the data has too much scatter. If the clouds are segregated by height, determinations of the long-wavelength sensitivity, G_L, of the cloud types become reliable. However, grouping clouds by height alone does not yield a meaningful measure of the SW sensitivity, G_S, or the net sensitivity, δ. The SW sensitivity is better estimated when clouds are classified by their OD. When the clouds were further subdivided by height and OD reasonably good estimates of G_L, G_S and δ were obtained.

We compared our results to model derived values. Some results confirmed certain obvious beliefs about the radiative effects of clouds. For example, high clouds can have up to an order of magnitude more effect on the long-wavelength at the TOA than lower clouds. It was also determined that the variations in OD of clouds (even at the same height) can alter the SW sensitivity by as much as two orders of magnitude (compare optically thick cirro-stratus clouds to cirrus). Although some of our results disagreed with model predictions. Analysis of the data suggests that clouds whose tops are above 440 mb have a net warming affect, while the model shows that depending on optical thickness some high clouds can have a net cooling effect.

II. DATA

The analysis was performed on satellite data which was collected over Indonesia (10S to 10N and 90E to 150E) shown in Figure 1. The months selected were June and July of 1985 and 1986. This region and period was selected for its well known convective activity which creates a variety of cloud types [*Murakami*, 1983]. The time period was selected because these are months of intense

convective activity and 1985 and 1986 contain coincident observations of the two satellite systems used (described below).

The Earth Radiation Budget Experiment (ERBE) is a system of satellites which began measuring the *ERB* in 1985 [*Barkstrom et al.*, 1989]. There are three active satellites: two polar orbiting (NOAA-9 and NOAA-10) and one with an orbit inclined at 56° (ERBS). The data we employed from ERBE was collected by the narrow field-of-view scanners of NOAA-9 and ERBS [*Smith et al.*, 1986]. The spatial resolution of a pixel is ~40 km and each pixel is gridded into a 2.5° × 2.5° grid. From the S-4 level of processing [*ERBE S-4 USERS GUIDE*, 1985] we retrieved observations of SW, OLR and the total albedo α_T. The two operational satellites (ERBS and NOAA-9) observe each position about two or three times a day. A model assimilates these observations into a 24 hour time series [*Brooks et al.*, 1986]. Then the observations and the modelled results are averaged to provide a monthly average for every hour at each grid box.

The International Satellite Cloud Climatology Project (ISCCP) began inferring cloud properties from measured radiances in 1983 [*Schiffer and Rossow*, 1983]. It is based on observations by the global network of geostationary satellites and at least one polar orbiting NOAA satellite. The region we selected was primarily viewed by the Japanese GMS-3 [*Rossow et al.*, 1988]. We utilized ISCCP C-2 processed data [*Rossow and Walker*, 1991], which is the monthly averages of three-hour time bins. ISCCP's cloud detection algorithm is described in Appendix I.

From the ISCCP C-2 data set we selected the cloud fractions for seven different classifications of clouds by cloud top height and visible optical depth (see Figure 2). The data is only provided for daylight hours because the visible reflectance is required to determine the optical depth. The fraction of each cloud type is the ratio of the number of pixels of a particular cloud type to the total number of pixels within a 2.5° × 2.5° region.

Each 2.5° × 2.5° grid box contains the monthly averages of both ERBE radiation values for each hour of local time and ISCCP cloud fractions for each three-hour period during daylight. In order to put both data sets on the same time scale the ISCCP data was converted from GMT to local time. Then the three ERBE hourly data points around each ISCCP data point were averaged. For example, if the longitude of a data point is 120°E and the ISCCP data is reported for 0300 GMT, then this corresponds to 1100 local time. The ERBE data for 1000, 1100 and 1200 are averaged and all analysis is done in terms of local time and the ERBE average. Much of the ERBE temporal resolution is due to model-based interpolation, while the ISCCP data is provided by geostationary satellites which continously view the earth. For this reason, we decided to smooth the ERBE data rather than interpolate the ISCCP data.

The total region (20° in latitude by 60° in longitude) is divided into 8 × 24 boxes. The region is then divided into six longitude zones 10° wide and 20° in latitude (8 × 4 boxes in each zone). This subdivision is a compromise between using large numbers of points to get 'better' statistics and analyzing a geographically distinct and uniform region. Since cloud radiative effects depend on surface conditions and local meteorlogical conditions, performing a regression over too large an area or over too long a time span will not provide an accurate picture of any particular scene. Typically there are 3 values for each zone (e.g. 0900, 1200, 1500 local time) depending on how many daylight observations are reported by ISCCP. There are four months of data (June and July of 1985 and 1986). In all there are 80 separate cases (four months and each month contains six zones and each zone has reported data between three and four times). Each case is analyzed (see below) separately and the results are then compared.

III. ANALYSIS

We Start from the equations describing the radiative flux measured by the satellite at the TOA:

$$OLR = F_o(1-f) + F_c f = F_o + (F_c - F_o)f. \tag{5}$$

$$SW \simeq S_\odot \mu \alpha_o (1-f) + S_\odot \mu \alpha_c f = S_\odot \mu \alpha_o + S_\odot \mu (\alpha_c - \alpha_o) f. \tag{6}$$

$$N = S_\odot \mu - SW - OLR, \tag{1}$$

where OLR is the IR flux, F_o is the clear sky flux and f is the cloud fraction. In (6) SW is the visible flux, $S_\odot$ is the solar flux, μ is the cosine of the solar zenith angle. α_o and α_c are the surface and cloud albedoes respectively. Equations (5) and (6), and by extension (1), suggest that there is a linear relation between cloud fraction and radiative flux. In the spirit of *Ohring and Clapp* [1980], we plotted flux (ERBE) observations against cloud fraction determinations (ISCCP) and calculated least-squares regression lines and correlation coefficients. In Figure 3 an example is given of a particular case. This case was selected because it had the highest correlation coefficient for the NET case, and there is somewhat less scatter than a typical case. The distribution of the adjusted correlation coefficients ($\Re^2$) is shown in Figure 5 and the median value is presented in Table 1. The adjusted correlation coefficient is explained in Appendix II.

One of the fundamental criticisms of this approach is its assumptions that the optical properties of clouds are uniform. That is, if you decrease the fraction of warm, low clouds this will have the same radiative effect as a similar decrease in cold, high clouds. Since this is not believed to be true, we can segregate clouds by height and perform an analogous investigation. From equations (1), (5) and (6) we have:

$$OLR = F_o + G_L^H f^H + G_L^M f^M + G_L^L f^L. \tag{7}$$

$$SW = S_\odot \mu \alpha_o + G_S^H f^H + G_S^M f^M + G_S^L f^L. \tag{8}$$

$$N = S_\odot \mu (1-\alpha_o) - F_o + \delta^H f^H + \delta^M f^M + \delta^L f^L. \tag{9}$$

The superscripts H, M and L refer to the heights of the cloud tops and their respective sensitivities. The actual distinctions based on pressure-height are defined by ISCCP to be: $H < 440$ mb, 440 mb $< M < 680$ mb and $L > 680$ mb. The slopes and multi-variate adjusted correlation coefficients ($\Re^2$) were calculated for each case separately by multi-variate least-squares analysis [*Bevington*, 1969]. As an example of multi-variate analysis from the long-wavelength case, we solved for the variables G_L^H, G_L^M, and G_L^L which minimizes the following equation:

$$\chi^2 = \sum (OLR - F_o - G_L^H f^H - G_L^M f^M - G_L^L f^L)^2, \tag{10}$$

where F_o is a constant, dependant on the fitted slopes and sum is over the grid boxes in the zone (typically 32). The distribution of the adjusted correlation coefficients ($\Re^2$) is shown in Figure 5 and the median value is presented in Table 1. The high-cloud sensitivities, G_L^H, G_S^H and δ^H are plotted in Figure 4 as a function of local time. The error bars show the variance of the mean of the derived slopes for that particular hour, and assuming there is no instrumental uncertainty. The error bars for the NET curve were omitted for clarity, but they were comparable in size to the error bars associated with the SW curve. The curves were smoothed by a box-car function of 3. The

sensitivities obtained for the mid and low level clouds showed more variability and had larger error bars.

In a similar vein, the clouds were grouped into three classifications by optical depth (see Figure 2), and the same analysis was performed. The distribution of the adjusted correlation coefficients ($\Re^2$) is shown in Figure 5 and the median value is presented in Table 1. The median and distribution of the adjusted correlation coefficient was approximately the same for the OLR and NET cases as it was for the previous analysis, based on cloud height. However, the median $\Re^2$ for the SW case improved by 18% over the cloud-height based analysis and 51% over the total cloud fraction value. This improvement indicates that the measured SW flux is better fit by a linear model of clouds which are distinguished by OD, rather than height.

Segregating clouds based on their height improves the confidence with which we derive the IR radiative properties of clouds, and segregating clouds based on their optical depth allows us to better estimate the clouds' SW properties. Neither classification can adequately account for the clouds' NET effects. However, if clouds are classified based on both their height and OD then the NET sensitivities can be determined. The seven cloud types are described in Figure 2. A multi-variate least-squares fit was performed on each region for the OLR, SW and NET fluxes. The only difference between this regression and that shown in equations (7), (8) and (9) was that there were seven variables included in the fit. A sensitivity was obtained for each cloud type with respect to each flux. These results were weighted by the uncertainty of the fitted slope and averaged [*Bevington*, 1969]. The distribution of the adjusted correlation coefficients ($\Re^2$) is shown in Figure 5 and the median value is presented in Table 1. In Table 2 the averages of the cloud sensitivities are presented with the quoted errors being the variance of the mean.

IV. MODEL ANALYSIS

A one-dimensional radiative model was used to derive the cloud sensitivities in order to compare them to observations. The model is described in *Chou et al.* [1991] and *Chou* [1990]. The clouds in the model are parameterized in terms of the pressure of their top and base, optical thickness and fractional coverage. The model was run with a standard tropical atmosphere and a surface temperature of 300K at a resolution of 123 pressure levels, although only the flux at the TOA was analyzed. It was run for solar conditions at each hour from 0700 until 1200 of July 1 over the equator. The surface albedo was set at 0.6 at 0700 and was decreased by 0.1 at each hour until it was 0.1 at 1200.

Seven cloud types were specified to roughly correspond to the definitions given by ISCCP, although little effort was made to maximize the similarities between the model and the observations by adjusting the cloud properties. The input parameters are summarized in Table 3. The cloud fractions of the lower cloud types are increased by a random overlap scheme to account for underestimates by the satellite observation. For each hour that the model was run, the fraction of each cloud type was increased by 1%. Then it was reset to its original value. By subtracting the reference results from the altered cloud fraction results, the equivalent of $\frac{\Delta F}{\Delta f_i}$ is calculated, where F is either the OLR or SW flux, f_i any type of cloud and Δf_i is 1%. This ratio is the sensitivity of that radiative component (G_L or G_S) with respect to a particular type of cloud. With the observations the net flux was calculated and the regressions was performed separately, although with the model δ was obtained by adding G_L and G_S for each cloud type. Each sensitivity was calculated for each hour between 0700 and 1200, then assuming that the day is symetric about 1200, we averaged these results to compare with the observations. The model results are given in Table 4.

V. CAUTIONS

There are several major caveats to be mentioned before conclusions can be drawn from this analysis. The first is that the analysis is of limited geographical and temporal extent. Strictly speaking, generalizations to other seasons and geographies should be made cautiously. Secondly, our analysis compared monthly averaged fluxes and cloud data. This was done to reduce the scatter introduced by daily or synoptic fluctuations in the weather. The linear regression fits we obtained apply to monthly averaged values and it would be statistically incorrect to use them to predict instantaneous fluxes, although this is essentially what was done when comparing our results to the model's.

An additional concern is the relationship between cloud sensitivity and the concept of 'cloud forcing' [*Ramanathan et al.*, 1989]. It is tempting to translate the values of the cloud sensitivity into estimates of cloud forcing. The customary method would be to multiply the sensitivity by the cloud fraction. However, in this case it is probably not appropriate. The slopes calculated should be interpretted as what change would be expected in the average radiative flux for a small perturbation in the average cloud fraction. To justify this view we note that there is often disagreement between the reported clear-sky fluxes and the calculated intercept by the linear regression method. This discrepancy can be explained by noting that the sensitivities depend on the overall cloud-coverage, hence the fluxes are not entirely linear over the entire range of cloud coverage. For example a 90% change in cloud fraction will probably not have a 90 times greater effect on the radiative fluxes as a 1% change. In other words, these regression lines should not be extrapolated to regions beyond the extent of the data and since we are dealing with monthly average cloudiness, there were no regions with near-zero percent cloudiness.

Even though the short-wave and net sensitivities are known to have a strong diurnal signal (Figure 4), this was not factored into the average values. These are averages of daytime only. There is little diurnal variation of the IR flux, but the SW flux is zero at night. The daily average of the SW sensitivity might be half of the value reported here, since this average was not weighted with the hours of darkness. The NET sensitivity is also not weighted to account for the lack of SW radiation at night, so clouds probably have a stronger warming effect than what is reported here. The reason why the analysis can not be performed at night with the OLR data is because the cloud identification in terms of optical depth requires the visible reflection.

We have implicitly assumed that the ERBE fluxes are error free. They probably have smaller intrinsic errors ($\sim$5 W m^{-2}) than the cloud fraction data. This is, in part, due to the more difficult task of processing radiative data into cloud fractions, rather than reporting the radiance which is closer to direct measurement. If we assume the cloud fraction determination has an error of around 10% and a mean coverage of 60%, the error introduced into the sensitivity calculations can be estimated [*Bevington*, 1969]. This (instrumental) error is smaller than the error in slope determination caused primarily by scatter observed in the data. For this reason, we neglect quoting contributions to the uncertainty due to errors in the flux averages or cloudiness values. It is the high spatial and temporal variability of clouds which creates the scatter and makes their effects difficult to calculate.

Finally, it should be made clear that this is not a regression against height or optical depth. The clouds are grouped by their height or optical depth or both, then the regression is performed against the fractional cloud coverage of that group. In other words, we are determining the sensitivity of the radiation budget components, with respect to fractional cloud coverage of clouds with a specific

optical depth or height range.

VI. DISCUSSION

Table 1 summarizes the importance of different cloud properties in attempting to estimate their effects on the radiative fluxes at the TOA. That is, variations in cloud fraction alone explain only 21% of the variations in the measured net radiation. This implies that even if we knew whether cloudiness would increase or decrease due to changes in the concentration of greenhouse gases, this information would not be adequate for predicting corresponding changes in the ERB due to the change in cloud coverage.

If the clouds of different heights are treated separately in a linear regression the explained variance of the OLR is improved (from 66% to 87%). This is in contrast to the improvement of the SW and NET regressions. Although the regression against NET was increased by a larger percentage, the degree of confidence is still low. The conclusion is that cloud height is a critical parameter in estimating the effects of clouds on OLR. In particular, changes in the high cloud fraction were observed to have a more significant impact on the OLR than changes in either mid or low clouds. Not only was the magnitude of the sensitivity higher, but the relative uncertainty in the determination of the slope was lower. This result confirms the belief that high clouds have a dominant role in regulating the OLR.

When the optical depth (as calculated from the visible brightness) is introduced as a means of classifying cloud types (Figure 2) then the SW flux data can be better correlated with the cloud coverage data. In particular, optical depth-defined cloud types yield a better linear description of the SW flux then either total cloud fraction or height segregated clouds. The OLR regression against OD defined clouds, rather than height defined clouds, only slightly decreases the median adjusted correlation coefficient. The NET regression shows only a slight improvement over the height-only analysis.

When the optical depth and cloud height are used to discriminate cloud types (Figure 2) then the flux data can be better correlated with the cloud coverage data. This is especially noted in the regression against N. In this case the median $\Re^2$ increased by 14% over the best three cloud-type fit. This improvement suggests that both optical depth and cloud height information are required in order to expect a linear relationship between a certain cloud type and the net flux. The explained variance for the SW fit increased by 6% compared to the optical depth regression. Likewise, the OLR regression improved by only 7% compared to the height derived correlation coefficients. These small increases show that the addition of cloud height or optical depth information for the OLR or SW regressions respectively do not greatly improve the quality of the fit. This confirms the belief that most of the relevant information about the radiative effects of clouds on the OLR (SW) is cloud height (OD).

Upon comparison, the model and observational results have some similarities and also some notable discrepancies. The model treats all clouds as optically opaque to IR radiation. Their derived long wavelength sensitivity is mostly a function of the height of their tops, and weakly of the height of their bases. The observations do not support the assumption that all clouds are opaque to IR. The cirrus clouds, which were expected to have the strongest effect on the OLR, were observed to have a weaker effect then the cirro-stratus or convective clouds. A possible explanation is that transmission of IR flux through the cloud diminishes their effect. Another possible explanation is that high, thin cirrus clouds were overlapping lower optically thick clouds. This would cause cirrus clouds to be mis-classified as cirro-stratus or convective clouds. The positive long wavelength

sensitivity of the stratus and cumulus clouds is enigmatic. There are two possible explanations for this: 1) Due to cloud overlap or irregular surface conditions or poor contrast between the surface and clouds, the low cloud coverage is not measured as accurately as the upper clouds are measured; 2) A second possibility is that these clouds are associated with shallow convection, so that their formation is observed under conditions where warm air is convectively raised and cools [*Soong and Ogura*, 1980]. In this case, increased cloudiness of this type would be observed with an increase in the OLR.

In the SW, the OD has a critical effect on the sensitivity. The most serious discrepancy between the model and observational results is for the convective cloud. The model predicts that the convective clouds (optical depth of 30) will have a SW sensitivity almost 50% higher than observations indicate. There are several possible explanations. When extremely bright clouds are present the ERBE model might consistently under-estimate the SW flux since peak reflectance is probably not observed directly due to limited daily observations [*Brooks et al.*, 1986]. Another possibility is that the model does not account for any geometric effects of the cloud. These clouds are tall towers, and not plane-parallel clouds as the model assumes. The sensitivity of the cumulus clouds determined from the observations is strong and of the opposite sign from what is expected. Since this cloud type also gives anamolous results in the long wave-length analysis, the determination of the sensitivities are probably not reliable either because of inaccurate cloud identification or un-accounted for meteorological conditions.

The NET sensitivity determination is the least certain, although most important in assessing the effect of clouds on the climate. The observations indicate that all high clouds have a net warming effect on the climate, while the model shows that the optically thick convective clouds have a net cooling effect. It is these deep convective clouds, which are both optically thick and have high, cold tops which typify the difficulty in determining the net sensitivity. The quantity we wish to evaluate is the small difference between two large competing effects. For the mid level clouds, both observations and the model show that optically thick clouds cool and thin clouds warm the earth. What is unexpected is that the observational result seems to magnify the effect so that the net sensitivities of the mid level clouds are larger than either the long or short wavelength sensitivities. The low optically thick stratus clouds have a strong cooling effect on the net radiation. The low optically thin clouds have a weak cooling effect, although results derived by the long and short wavelength observations separately are opposite in sign to what was expected. Additionally, the uncertainty associated with this result is 114%.

The differences between the observations and the model are not totally unexpected. The cloud parameterization is very crude in the model, and there are still several key approximations involved in the cloud detection scheme (i.e. Partially filled pixels, cloud overlap effects, the setting of a threshold, etc...). One hope is that this type of study will be used to test and improve cloud parameterization. For example, can the observations be duplicated by the model better if quantities such as the emissivity of cirrus clouds were a free parameter? Without specific observational studies, there is little constraint on the quality of the model.

It is not surprising that there are correlations between radiation measurements and cloud data. After all, the cloud data itself was derived from radiation measurements. The main result is that cloud fraction alone is insufficient information to calculate the sensitivity of radiation components to cloud coverage. However, if the cloudiness can be described in terms of the heights of clouds for IR sensitivity and optical depth for the solar sensitivity, then the sensitivities can be determined

with adequate precission.

APPENDIX I - ISCCP's cloud detection algorithm from *Rossow et al.*[1988]

Cloud detection is difficult and controversial, however, ISCCP provides the best available uniform global cloud data [*Rossow et al.*, 1985]. ISCCP first measures or infers the clear-sky conditions of both the infrared (IR) and visible (VIS) channels. Then, depending on the type of surface (i.e. land, sea, coast, or 'high-variability' land) thresholds are established for both channels which is a measure of the variation expected of that surface. The pixel radiances are compared to the clear-sky radiances and are given a VIS and an IR code number (from 0-5) depending on how they differ from the clear-sky case. A 6×6 grid of VIS and IR code numbers designates whether the pixel is clear, cloudy or undecided. For example, over the ocean (surface type 1), the IR threshold is 2.5K and the VIS threshold is 3.0%. If a pixel is 4K colder than the clear-sky case it is given an IR code number 4 (colder by an amount between 1 and 2 times greater than the threshold). And if the VIS radiance is 8% greater than the clear-sky case the pixel is given a VIS code number of 5 (brighter by more than 2 times the threshold). According to the grid a pixel with a VIS code of 5 and an IR code of 4 is cloudy.

Once a pixel is classified as cloudy, its heigth is estimated by comparing is brightness temperature with a measured temperature profile. Then the optical depth of the cloud is estimated. This is done by assuming that the light reflected from clouds due to multiple Mie-scattering by spherical water drops with an effective radius of 10 μm with a variance of 0.15 μm. If the optical depth is low, the cloud height is adjusted to account for transmission of surface IR radiation.

APPENDIX II - The Adjusted Correlation Coefficient $\Re^2$

We begin with the equation relating the radiative flux F to the cloud fraction f:

$$F = A + Gf. \tag{A.1}$$

G and A are calculated to minimize

$$\chi^2 = \sum (F - Gf - A)^2, \tag{A.2}$$

where the sum is over N co-incident measurements of F and f. The correlation coefficient r is defined from *Bevington* [1969]:

$$r \equiv \frac{N \sum Ff - \sum f \sum F}{[N \sum f^2 - (\sum f)^2]^{1/2} [N \sum F^2 - (\sum F)^2]^{1/2}}, \tag{A.3}$$

which ranges from -1 to +1. If r is near zero, it implies little correlation between the two variables and if r is close to either -1 or +1 it signifies a good linear fit. Conventionally r is squared, and this is defined to be the explained variance. If A.1 is generalized to include K independent variables, the other equations can also be generalized:

$$F = A + \sum_{j=1}^{K} G_j f_j, \tag{A.4}$$

where j is the cloud type. R^2 is the squared multi-variate form of the single-variable linear correlation coefficient r. It is a measure of the 'goodness of fit' of the function of the variables f_j to F. It is defined in *Judge et al.* [1980] to be:

$$R^2 = 1 - \frac{(\sum F - A - \sum G_j f_j)^2}{(\sum (F - \overline{F}))^2}, \tag{A.5}$$

where $\overline{F}$ is the mean value. The problem with R^2 as a critereon for the goodness of fit is that it typically increases with more independent parameters. The adjusted correlation coefficient accounts for the increase in free parameters, so that the adjusted correlation coefficient derived with three independent variables (cloud height) can be compared to a fit made with seven independent variables (cloud height and optical depth). Adjusted correlation coefficients can be compared independently of K. It is defined in *Judge et al.* [1980] to be:

$$\Re^2 = 1 - \left(\frac{N-1}{N-K}\right)(1 - R^2). \tag{A.6}$$

REFERENCES

Ardanuy, P.E., L.L. Stowe, A. Gruber, and M. Weiss, 1989, Shortwave, Longwave and Net Cloud-Radiative Forcing as Determined from Nimbus-7 Observations, *J. Geophys. Res.*, submitted.

Arking, A., 1991, The Radiative Effects of Clouds and their Impact on Climate, *Bull. Amer. Meteor. Soc.*, in press.

Barkstrom, B., E. Harrison, G. Smith, R. Green, J. Kibler, R. Cess, and the ERBE Science Team, 1989, Earth Radiation Budget Experiment (ERBE) Archival and April 1985 Results, *Bull. Amer. Meteor. Soc.*, **70**:1254-1262.

Bevington, P.R., 1969,*Data Reduction and Error Analysis for the Physical Sciences*, McGraw-Hill, New York.

Brooks, D.R., E. F. Harrison, P. Minnis, J.T. Suttles, R.S. Kandel, 1986, Development of Algorithms for Understanding the Temporal and Spatial Variability of the Earth's Radiation Balance, *Rev. Geophys.*, **24**:422-438.

Chou, M-D., D.P. Kratz, W. Ridgway, 1991, IR Radiation Parameterizations in Numerical Climate Models, *J. Climate*, **4**:424.

Chou, M-D., 1990, Parameterizations for the Absorbtion of Solar Radiation by O_2 and CO_2 with Application to Climate Studies, *J. Climate*, **3**:209-217.

ERBE S-4 USERS GUIDE, 1985, ERBE Data Management Team, ERBE 3-3-12-3-85-1-10.

Judge, G.G., W.E. Griffiths, R.C. Hill, H. Lütkepohl, T-C. Lee, 1980, *The Theory and Practice of Econometrics*, 2nd ed., Wiley, New York, pp. 862-3.

Hartmann, D.L., V. Ramanathan, A. Berroir, G.E. Hunt, 1986, Earth Radiation Budget Data and Climate Research, *Rev. Geophys.*, **24**:439-468.

Hartmann, D.L., D.A. Short, 1980, On the Use of Earth Radiation Budget Statistics for Studies of Clouds and Climate, *J. Atmos. Sci.*, **37**:1233-1250.

Hartmann, D.L., D. Doelling, 1991, On the Net Radiative Effectiveness of Clouds, *J. Geophys. Res.*, in press.

Minnis, P., E.F. Harrison, 1984, Diurnal Variability of Regional Cloud and Clear-Sky Radiative Parameters Derived from GOES Data. Part I: Analysis Method, *J. Clim. Appl. Met.*, **23**:993-1011.

Murakami, M., 1983, Analysis of the Deep Convective Activity Over the Western Pacific and Southeast Asia,*J. Met. Soc. Japan*, **61**:60-75.

Ohring, G., P. Clapp, 1980, The Effect of Changes in Cloud Amount on the Net Radiation at the Top of the Atmosphere, *J. Atmos. Sci.*, **37**:447-454.

Ramanathan, V., R.D. Cess, E.F. Harrison, P. Minnis, B.R. Barkstrom, E. Ahmad, D. Hartmann, 1989, Cloud-Radiative Forcing and Climate: Results from the Earth Radiation Budget Experiment, *Science*, **243**:57-63.

Rossow, W.B., A.W. Walker, 1991, The International Satellite Cloud Climatology Project (ISCCP) Discription of Monthly Mean Cloud Data (Stage C2), World Meterological Organization / International Council of Scientific Unions.

Rossow, W.B., L.C. Gardner, P-J. Lu, A. Walker, 1988, The International Satellite Cloud Climatology Project (ISCCP) Documentation of Cloud Data, WMO/TD-No. 266, World Meterological Organization / International Council of Scientific Unions.

Rossow, W.B., F. Mosher, E. Kinsella, A. Arking, M. Desbois, E. Harrison, P. Minnis, E. Ruprecht, G. Seze, C. Simmer, and E. Smith, 1985, ISCCP Cloud Algorithm Intercomparison, *J. Clim. Appl. Met.*, **24**:877-903.

Schiffer, R.A., W.B. Rossow, 1983, The International Satellite Cloud Climatology Project (ISCCP): The First Project of the World Climate Research Programme, *Bull. Amer. Meteor. Soc.*, **64**:779-784.

Schneider, S., 1972, Cloudiness as a Global Climatic Feedback Mechanism: The Effects on the Radiation Balance and Surface Temperature of Variations in Cloudiness, *J. Atmos. Sci.*, **29**:1413-1422.

Smith, G.L., R.N. Green, E. Raschke, L.M. Avis, J.T. Suttles, B.A. Wielicki, R. Davies, 1986, Inversion Methods for Satellite Studies of the Earth's Radiation Budget: Development Algorithms for the ERBE Mission, *Rev. Geophys.*, **24**:407-421.

Soong, S-T., Y. Ogura, 1980, Response of Tradewind Cumuli to Large-Scale Processes, *J. Atmos. Sci.*, **37**:2035-2050.

Table 1. The median adjusted correlation coefficients ($\Re^2$). The column labels refer to how the clouds were classified. f is no classification (total cloud fraction); H is the results when the clouds were segregated by Height; OD is from classification based on optical depth; H & OD is when clouds were defined by both their Height and optical depth.

	f	H	OD	H & OD
LW	0.666	0.869	0.863	0.932
SW	0.521	0.665	0.789	0.839
NET	0.207	0.638	0.679	0.789

Table 2. Determinations of the sensitivities by different cloud type (see Fig. 2). Each case was analyzed separately, and the results were averaged. The averages were weighted by the uncertainty in their determination. The quoted errors are the variance of the mean. The larger errors associated with the SW and NET determinations reflect variation due to the diurnal cycle and uncertainty in fitting the data. The quoted errors do not include any instrumental error. Note that for the LW and SW slopes positive implies cooling and negative implies warming, while the NET case is reversed (positive implies warming).

CLOUD TYPE	LW	SW	NET
convective	-1.11 ± 0.03	1.93 ± 0.07	0.74 ± 0.10
cirrostratus	-1.52 ± 0.03	2.86 ± 0.10	1.01 ± 0.14
cirrus	-0.40 ± 0.03	0.37 ± 0.09	1.60 ± 0.13
nimbo-stratus	-0.18 ± 0.09	1.66 ± 0.22	-3.37 ± 0.32
altocumulus	-0.69 ± 0.05	0.55 ± 0.14	1.45 ± 0.21
stratus	0.11 ± 0.06	1.49 ± 0.16	-3.18 ± 0.24
cumulus	0.96 ± 0.07	-1.95 ± 0.19	-0.25 ± 0.29

Table 3. Cloud input parameters for the model.

CLOUD TYPE	TOP (mb)	BASE (mb)	OD	FRACTION (0–1)
convective	200	680	30	0.081
cirrostratus	150	440	15	0.125
cirrus	150	200	0.5	0.170
nimbo-stratus	550	680	10	0.030
altocumulus	550	680	2	0.056
stratus	825	1000	5	0.062
cumulus	825	1000	1	0.066

Table 4. Model results under the same sign conventions as in Table 2.

CLOUD TYPE	LW	SW	NET
convective	-1.6	3.0	-1.4
cirrostratus	-1.8	2.6	-0.9
cirrus	-1.8	0.0	1.8
nimbo-stratus	-0.5	1.8	-1.3
altocumulus	-0.5	0.5	0.0
stratus	-0.1	1.0	-0.9
cumulus	-0.1	0.1	0.0

Figure 1. Indonesia, divided into six 10° wide longitude zones.

Figure 2. ISCCP cloud classification based on height and optical depth from *Rossow and Walker* [1991]. The percentages of the mean coverage are listed in the boxes. The stars (*) are the positions of the tops and optical depths of the model input clouds. The shaded boxes are those classified as optically thick. The striped box intermediate and the unfilled boxes were considered thin.

Figure 3. The 'best-case' example of the regression of ERBE fluxes against total cloud fraction. This case was selected as an example because it showed the highest correlation of the NET with cloud fraction. Each 'case' represents 20° in latitude and 10° in longitude. Within that area there are 32 2.5° × 2.5° grid points. Each data point plotted is a monthly average of the flux and cloud fraction for a grid point for a specific hour (1700 local time in this case). This size region was selected because a larger region tended to introduce inhomogeneities which reduced the linearity of the fit, and smaller regions reduced the number of points, which decreased the significance of the fit. The correlation coefficients (r) were calculated for each case separately. They were converted to the adjusted correlation coefficient and then the median was selected. This indicates, on average, how well total cloud fraction serves as an predictor of variations in the flux.

Figure 4. Diurnal Variability of the SW, LW and NET sensitivities due to high clouds. Note that for the LW and SW curves positive values imply cooling and negative values imply warming. For the NET curve it is the opposite (positive is warming). The error bars are the variance of the mean for the values of the sensitivity at that hour. The error bars for the NET curve are omitted for clarity, although are comparable in size to those on the SW curve. All three curves were slightly smoothed.

Figure 5. The Distribution of the Adjusted Correlation Coefficient ($\Re^2$). Four months were analyzed separately and each month contained six longitude zones. Within each longitude zone there were either three or four analysis hours, depending on the reporting of cloud properties by ISCCP. Each of these analysis hours were analyzed separately and called a case. There were 80 cases in all (4 months x 6 zones x 3.3 times). This figure shows histograms of the $\Re^2$ binned into 20 bins of 0.05. The top row is regressions against the OLR, the middle row is against SW and the bottom row is against the NET. The column labels are the same as in Table 1.

Figure 1. Indonesia divided into six 10° wide longitude bins.

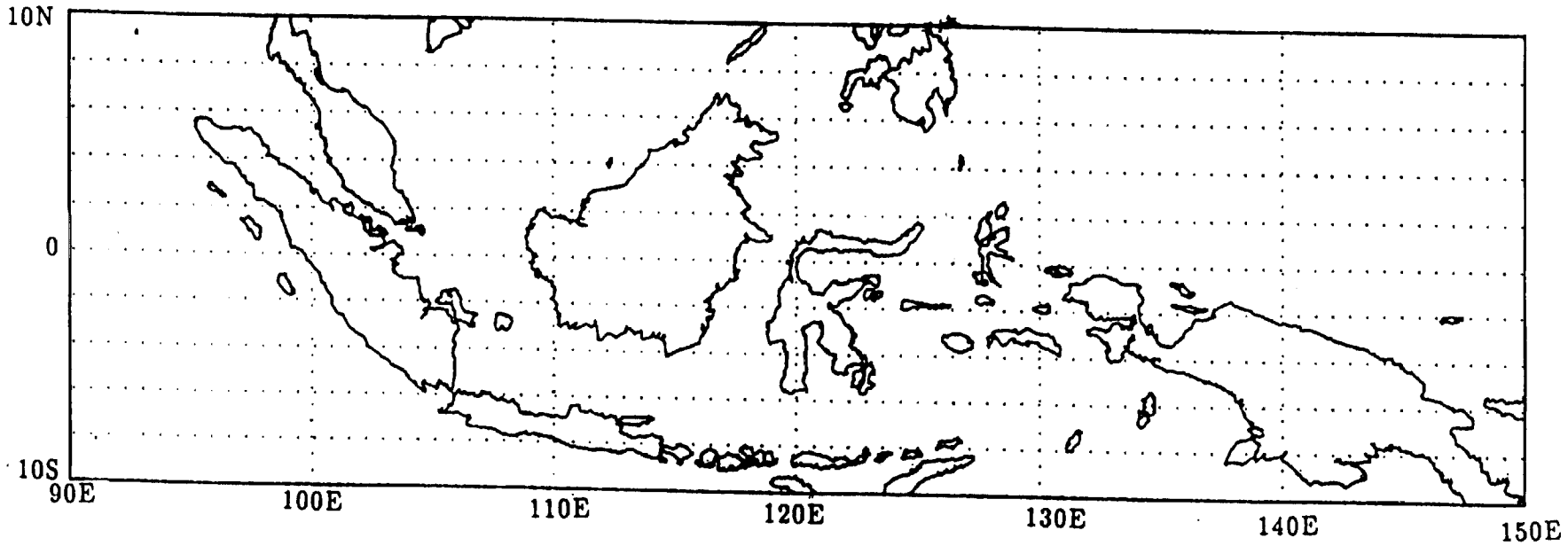

2. ISCCP Cloud Classification.

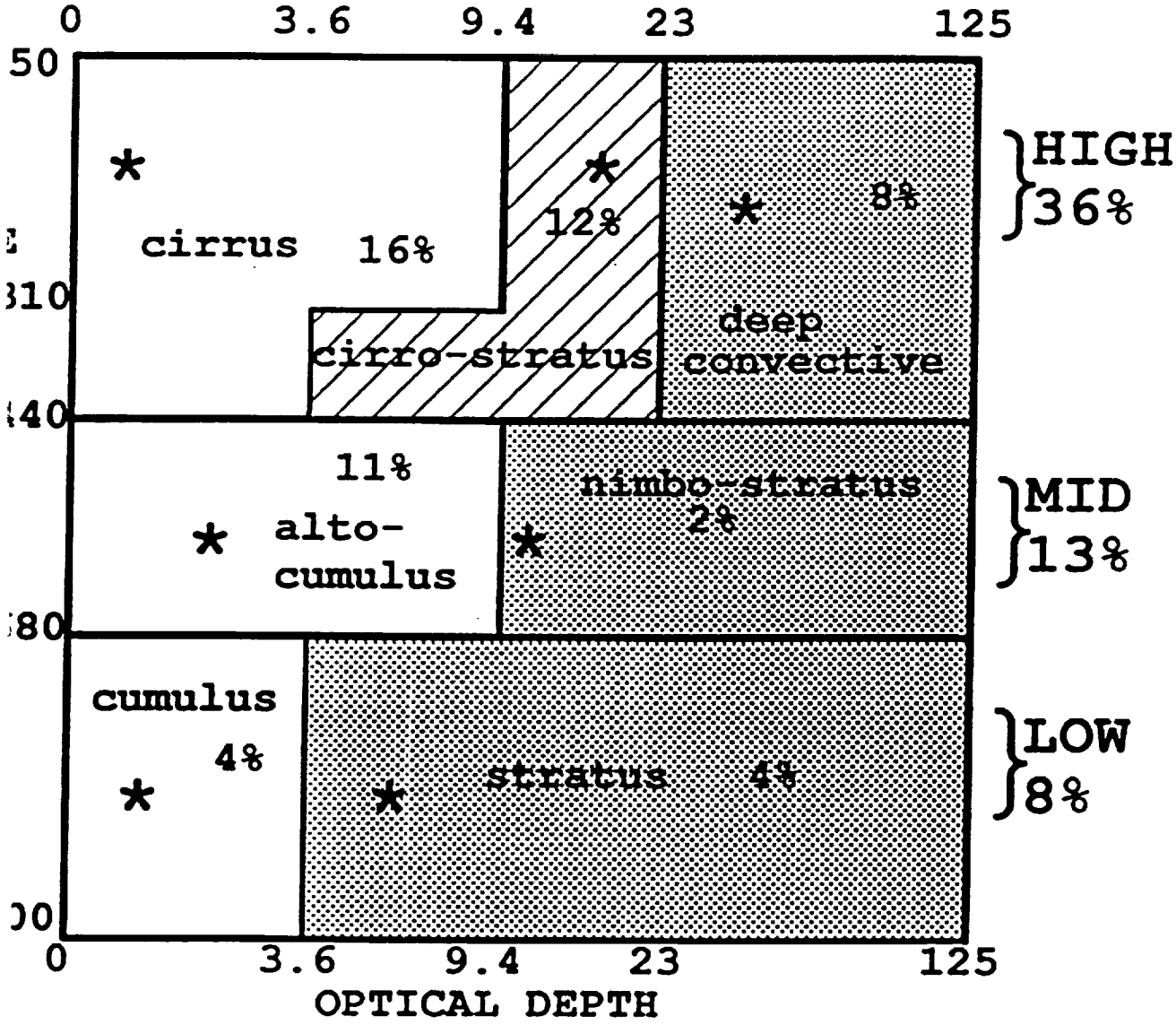

Figure 3. FLUX vs. CLOUD FRACTION
JUNE 1985, 1700 (lt)
10S–10N, 110E–120E

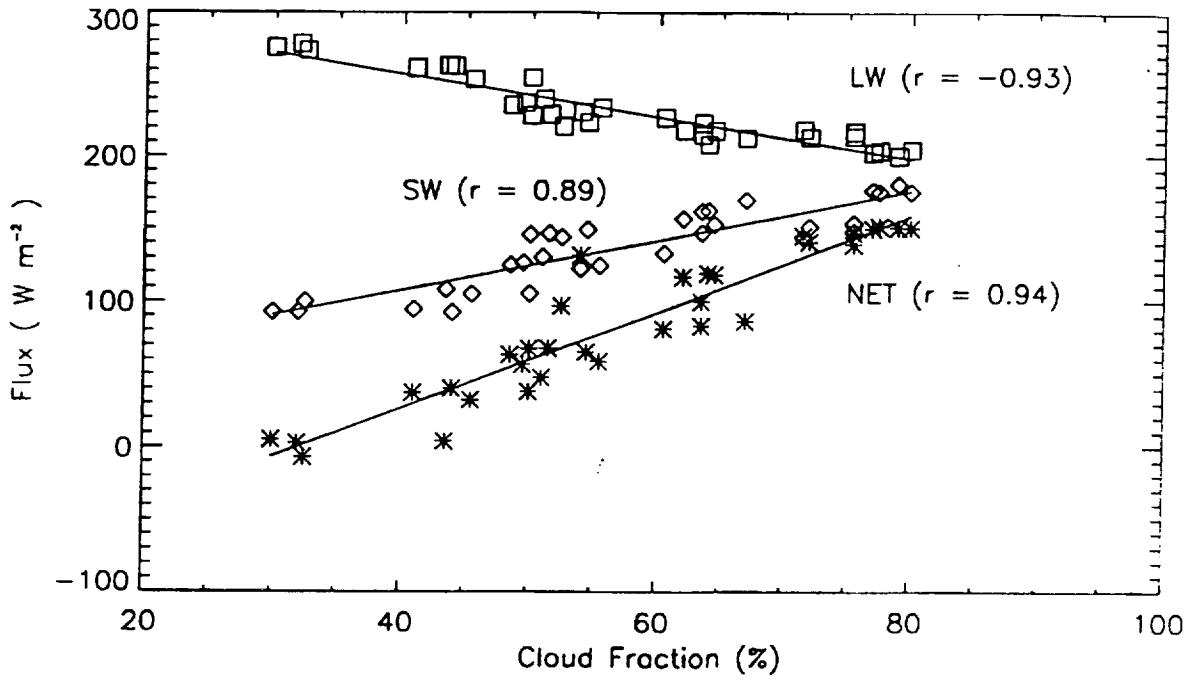

Figure 4. HIGH CLOUD SENSITIVITY

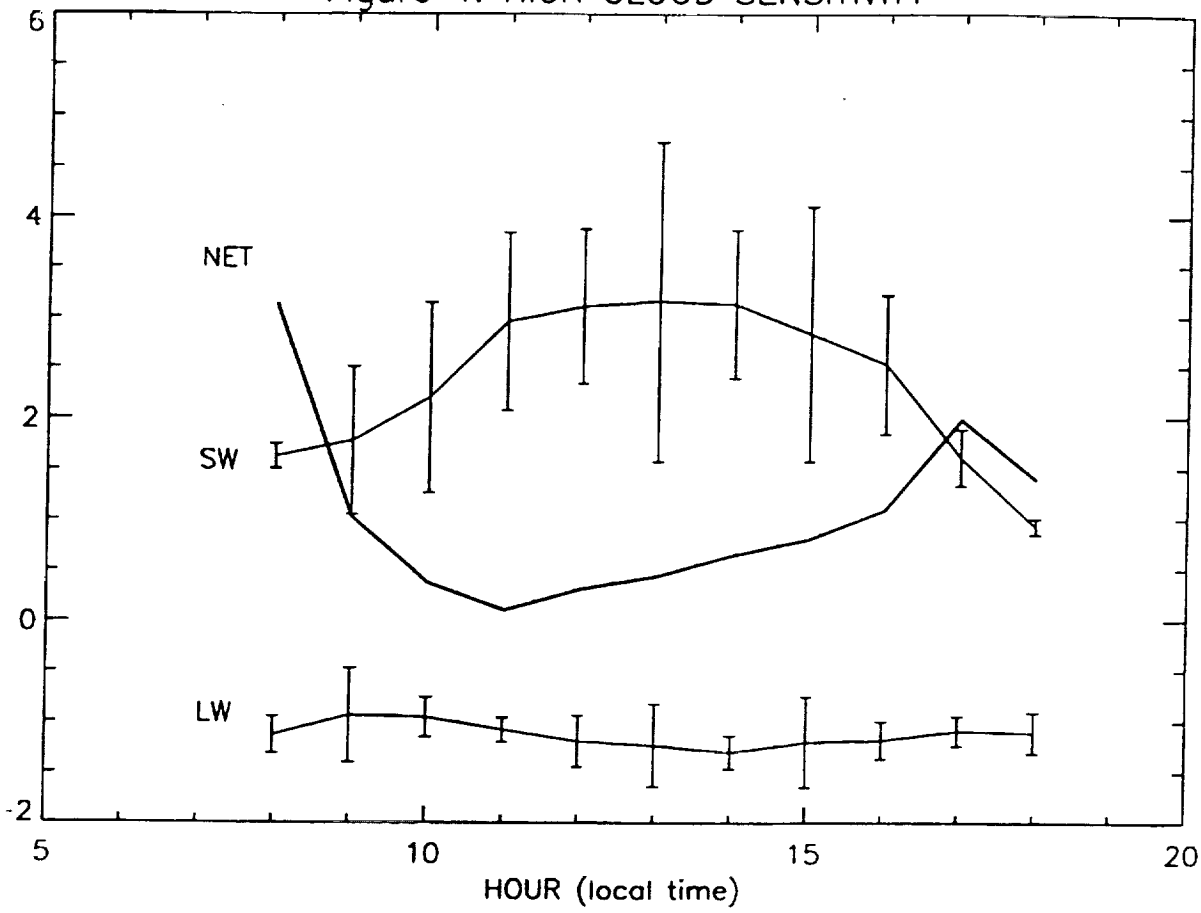

Fig. 5 Distribution of Adjusted Correlation Coefficients ($\bar{R}^2$)